Force Control of Redundant Robots in Unstructured Environment

Bojan Nemec and Leon Žlajpah

***Abstract*—In this paper, a method for force control of redundant robots in an unstructured environment is proposed. We assume that the obstacles are not known in advance. Hence, the robot arm has to be compliant with the environment while tracking the desired position and force at the end-effector. First, the dynamic properties of the internal motion of redundant manipulators are considered. The motion is decoupled into the end-effector motion and the internal motion. Next, the dynamic model of a redundant manipulator is derived. Special attention is given to the inertial properties of the system in the space where internal motion is taking place; we define a *null-space effective inertia* and its inverse. Finally, a control method is proposed which completely decouples the motion of the manipulator into the task-space motion and the internal motion and enables the selection of dynamic characteristics in both subspaces separately. The proposed method is verified with simulation and with experimental results of a four-degrees-of-freedom planar redundant robot.**

***Index Terms*—Compliance control, redundant systems, robot dynamics.**

I. Introduction

One of the important issues of the new generation of robotic manipulators is kinematic redundancy. Kinematic redundancy is characterized by extra degrees of freedom with respect to the given motion posed by the assigned primary task. A redundant manipulator has the ability to move the end-effector along the same task state using different configurations of the mechanical structure. This provides a means for solving sophisticated motion tasks such as avoiding obstacles, avoiding singularities, optimizing manipulability, minimizing joint torques, etc. The result is a significant increase in the dexterity of the system, which is essential to accomplish complex tasks. On the other hand, redundancy also has an important influence on the dynamic behavior of the robotic system. An appropriate control of dynamic properties is essential for higher performance in robotic manipulation. Most of the research in the field of the dynamics of robotic manipulators has been devoted to the dynamics in the joint space. To control the dynamic properties of the system in the joint space, different control methodologies have been proposed based on joint-space dynamic models [1], [11]. As the next step, methods have been proposed where the control takes place in the task space [12]. These methods include the transformations between joint-space trajectories and task-space trajectories. However, in the case of redundant manipulators, these transformations are not unique. Different methodologies have been proposed to resolve the redundancy, like optimization of a given performance criteria while satisfying a primary task [15].

Manuscript received July 6, 2000; revised July 16, 2001. Abstract published on the Internet December 5, 2001.

The authors are with the Department of Automatics, Biocybernetics and Robotics, Jožef Stefan Institute, 1000 Ljubljana, Slovenia (e-mail: bojan.nemec@ijs.si).

Publisher Item Identifier S 0278-0046(02)00916-4.

To overcome the limitations of control methods based on the joint-space dynamics methods, Khatib [8] proposed a method for dealing with dynamics and control in the task space. This method enables the description, analysis, and control of the robot behavior in the task space and can also be used for redundant manipulators when the dynamic behavior of the end-effector is of interest. However, for the redundant manipulators, the end-effector dynamics is only one part of the dynamics of the whole manipulator. The "rest" dynamics represent the dynamics of the internal motion of the manipulator. Recently, Park [16] proposed a decomposition of dynamics of kinematically redundant manipulators into the task-space dynamics and null-space dynamics based on a minimally reparametrized homogenous velocity.

The majority of the task posed to the robots requires interaction with the environment. Therefore, the ability to control the interaction forces is essential for a modern robot. In [14] we have proposed an approach to the force control of redundant robots. However, the proposed approach requires structured environment, where the position of the obstacles is known in advance or a complex sensory system is used to detect the environment obstacles. However, there are many situations where the obstacles are not known in advance or are changing position. An example of such a task could be working in a tube or working in a completely dark environment, where the vision sensors cannot be used. Humans solve such a situation by adapting the compliance of the arm. Our approach tries to imitate the human behavior in such a situation. This requires the study of the dynamic properties of the internal motion of redundant manipulators. We analyze what the causes are for the internal motion and how to use the internal motion to improve the performance of the overall system. Next, the influence of the selection of pseudo or generalized inverse on the internal motion is discussed and a method to derive the model describing the dynamics of the internal motion is presented. We define a *null-space effective inertia* and its inverse. Finally, impedance control method is presented, which completely decouples the motion of the manipulator into the task-space motion and the internal motion and enables the selection of dynamic characteristics in both subspaces separately.

II. Kinematics

The robotic systems under study are n-degrees-of-freedom (DOF) serial manipulators. We consider only the redundant systems which have more DOF than needed to accomplish the task, i.e., the dimension of the joint space n exceeds the dimension of the task space m, $n > m$. Let the configuration of the manipulator be represented by the vector $\boldsymbol{q}$ of n joint positions and the end-effector position (and orientation) by m-dimensional vector $\boldsymbol{x}$ of task positions (and orientations). The joint and task velocities are related by the following expression:

$$\dot{\boldsymbol{x}} = \mathbf{J}\dot{\boldsymbol{q}} \tag{1}$$

where $\mathbf{J}$ is the $m \times n$ manipulator Jacobian matrix. Mapping of joint velocities to the task velocities is unique, while mapping of the task velocities to the joint velocities is not. The general solution of (1) can be given as

$$\dot{\boldsymbol{q}} = \mathbf{J}^{\#}\dot{\boldsymbol{x}} + \mathbf{N}\dot{\boldsymbol{q}} \tag{2}$$

where $\mathbf{J}^{\#}$ is the generalized inverse of $\mathbf{J}$ and $\mathbf{N}$ is $n \times n$ matrix representing the projection of $\dot{\boldsymbol{q}}$ into the null space of $\mathbf{J}$, $\mathbf{N} = (\mathbf{I} - \mathbf{J}^{\#}\mathbf{J})$. The first term on the right side of (2) represents the part of the joint-space velocity necessary to perform the task and is denoted as $\dot{\boldsymbol{q}}_x$, $\dot{\boldsymbol{q}}_x = \mathbf{J}^{\#}\dot{\boldsymbol{x}}$. The second term denoted as $\dot{\boldsymbol{q}}_n$, $\dot{\boldsymbol{q}}_n = \mathbf{N}\dot{\boldsymbol{q}}$, represents the joint-space velocity due to the internal motion. Actually, $\dot{\boldsymbol{q}}$ in the second term of (2) can be an arbitrary velocity vector and is usually used to perform an additional subtask like optimization of different cost functions, obstacle avoidance, etc.

Differentiating (1), we obtain the relation between joint-space accelerations and task-space accelerations

$$\ddot{\boldsymbol{x}} = \mathbf{J}\ddot{\boldsymbol{q}} + \dot{\mathbf{J}}\dot{\boldsymbol{q}}. \tag{3}$$

Considering also the accelerations in the null space of $\mathbf{J}$, the general solution of (3) is typically given in the form

$$\ddot{\boldsymbol{q}} = \mathbf{J}^{\#}\left(\ddot{\boldsymbol{x}} - \dot{\mathbf{J}}\dot{\boldsymbol{q}}\right) + \mathbf{N}\ddot{\boldsymbol{q}}. \tag{4}$$

To be able to decompose the joint accelerations $\ddot{\boldsymbol{q}}$ into accelerations subjected to the task-space motion and to the internal motion, (4) has to be rewritten in the form

$$\ddot{\boldsymbol{q}} = \mathbf{J}^{\#}\ddot{\boldsymbol{x}} + \dot{\mathbf{J}}^{\#}\dot{\boldsymbol{x}} + \mathbf{N}\ddot{\boldsymbol{q}} + \dot{\mathbf{N}}\dot{\boldsymbol{q}}. \tag{5}$$

The above equation can also be obtained by differentiating (2). The first two terms on the right side of (5) represent the joint-space acceleration due to the task-space motion and the last two terms represent the joint-space acceleration due to the internal motion. The terms $\dot{\mathbf{J}}^{\#}\dot{\boldsymbol{x}}$ and $\dot{\mathbf{N}}\dot{\boldsymbol{q}}$ describe the accelerations due to the change in the configuration of the manipulator and are required to maintain the task-space and null-space velocity, respectively [13].

Similar decomposition exists also for the forces. For redundant manipulators, the relationship between the m-dimensional generalized force in task space $\boldsymbol{F}$ including linear forces and torques and the corresponding n-dimensional generalized joint-space force $\boldsymbol{\tau}$ is described by

$$\boldsymbol{\tau} = \mathbf{J}^T\boldsymbol{F} + \mathbf{N}^T\boldsymbol{\tau}_n \tag{6}$$

where $\mathbf{N}^T$ is $n \times n$ matrix representing the projection into the null space of $\mathbf{J}^T$ and $\boldsymbol{\tau}_n$ is an arbitrary n-dimensional vector of joint torques.

III. Selection of the Generalized Inverse

There is an infinite number of the generalized inverses $\mathbf{J}^{\#}$ which satisfy the equation

$$\mathbf{J}\mathbf{J}^{\#}\mathbf{J} = \mathbf{J}. \tag{7}$$

In the past, the Moore–Penrose pseudoinverse [10] has been widely used to resolve the redundancy. It is defined as

$$\mathbf{J}^{+} = \mathbf{J}^T\left(\mathbf{J}\mathbf{J}^T\right)^{-1}$$

where $n > m$. Its "weighted" counterpart [6] is defined as

$$\mathbf{J}^{+}_w = \mathbf{W}^{-1}\mathbf{J}^T\left(\mathbf{J}\mathbf{W}^{-1}\mathbf{J}^T\right)^{-1}$$

where $\mathbf{W}$ is an $n \times n$ weighting matrix. A special form of $\mathbf{J}^{+}_w$ is when $\mathbf{W} = \mathbf{H}$, where $\mathbf{H}$ is the inertia matrix of the manipulator. Khatib [9] has proven that

$$\bar{\mathbf{J}} = \mathbf{H}^{-1}\mathbf{J}^T\left(\mathbf{J}\mathbf{H}^{-1}\mathbf{J}^T\right)^{-1} \tag{8}$$

is the only pseudoinverse which is dynamically consistent, i.e., the task-space acceleration $\ddot{\boldsymbol{x}}$ is not affected by any arbitrary torques $\boldsymbol{\tau}_n$ applied through the associated null space, $\bar{\mathbf{N}}^T\boldsymbol{\tau}_n$, $\bar{\mathbf{N}}^T = (\mathbf{I} - \mathbf{J}^T\bar{\mathbf{J}}^T)$. Additionally, the dynamically consistent generalized inverse $\bar{\mathbf{J}}$ is the only generalized inverse which assures that an external force does not produce a null-space acceleration [5].

IV. Manipulator Dynamics

Assuming the manipulator consists of rigid bodies, the joint-space equations of motion can be written in a form

$$\boldsymbol{\tau} = \mathbf{H}(\boldsymbol{q})\ddot{\boldsymbol{q}} + \mathbf{C}\left(\boldsymbol{q}, \dot{\boldsymbol{q}}\right)\dot{\boldsymbol{q}} + \mathbf{g}(\boldsymbol{q}) - \boldsymbol{\tau}_E \tag{9}$$

where $\boldsymbol{\tau}$ is the n-dimensional vector of control torques, $\mathbf{H}$ is the $n \times n$ symmetric positive-definite inertia matrix, $\mathbf{C}(\boldsymbol{q}, \dot{\boldsymbol{q}})$ is the $n \times n$ matrix due to the Coriolis and centrifugal forces, and $\mathbf{g}$ is the n-dimensional vector of gravity forces. Vector $\boldsymbol{\tau}_E$ summarizes effects of all external forces acting on the manipulator.

Using the relation $\mathbf{I} = \mathbf{J}^T\mathbf{J}^{\#T} + \mathbf{N}^T$ and substituting (4) and (6) into (9), the model (9) can be rewritten in the form

$$\begin{aligned}\mathbf{J}^T\mathbf{F} + \mathbf{N}^T\boldsymbol{\tau} =& \mathbf{J}^T\mathbf{J}^{\#T}\left(\mathbf{H}\mathbf{J}^{\#}(\ddot{\boldsymbol{x}} - \dot{\mathbf{J}}\dot{\boldsymbol{q}}) + \mathbf{C}\dot{\boldsymbol{q}} + \boldsymbol{g} - \boldsymbol{\tau}_E\right)\\ &+ \mathbf{N}^T\left(\mathbf{H}\mathbf{N}\ddot{\boldsymbol{q}} + \left(\mathbf{C}\dot{\boldsymbol{q}} + \boldsymbol{g}\right) - \boldsymbol{\tau}_E\right)\\ &+ \left(\mathbf{J}^T\mathbf{J}^{\#T}\mathbf{H}\mathbf{N}\ddot{\boldsymbol{q}} + \mathbf{N}^T\mathbf{H}\mathbf{J}^{\#}(\ddot{\boldsymbol{x}} - \dot{\mathbf{J}}\dot{\boldsymbol{q}})\right).\end{aligned}$$

Note that the terms on the right side of the above equation are arranged into three groups. The first group includes the forces acting in the task space. The second group includes torques acting in the null space of $\mathbf{J}^T$. The third group represents the coupling forces and torques. To make the motion of the end-effector and the internal motion independent, it is necessary that the terms in the third group are always equal to zero

$$\mathbf{J}^{\#T}\mathbf{H}\mathbf{N} = \mathbf{N}^T\mathbf{H}\mathbf{J}^{\#} = \mathbf{0}. \tag{10}$$

The only value of $\mathbf{J}^{\#}$ which satisfies the condition (10) is $\bar{\mathbf{J}}$ as defined in (8).

The equation of the end-effector motion subjected to generalized task forces $\boldsymbol{F}$ is given in the form [8]

$$\boldsymbol{F} = \mathbf{M}(\boldsymbol{q})\ddot{\boldsymbol{x}} + \boldsymbol{\mu}(\boldsymbol{q}, \dot{\boldsymbol{q}}) + \boldsymbol{\gamma}(\boldsymbol{q}) - \boldsymbol{F}_E$$

where $\mathbf{M}$, $\boldsymbol{\mu}$, $\boldsymbol{\gamma}$ and $\boldsymbol{F}_E$ are, respectively, the $m \times m$ symmetric positive-definite matrix describing the inertial properties of the manipulator in the task space, the m-dimensional vector of Coriolis and centrifugal forces, the m-dimensional vector of gravity forces, and the m-dimensional vector of external forces, all acting in the task space

$$\begin{aligned}
\mathbf{M} =& \bar{\mathbf{J}}^T\mathbf{H}\bar{\mathbf{J}} = \left(\mathbf{J}\mathbf{H}^{-1}\mathbf{J}^T\right)^{-1} \\
\boldsymbol{\mu} =& \bar{\mathbf{J}}^T\mathbf{C}\dot{\boldsymbol{q}} - \mathbf{M}\dot{\mathbf{J}}\dot{\boldsymbol{q}} \\
\boldsymbol{\gamma} =& \bar{\mathbf{J}}^T\boldsymbol{g} \\
\boldsymbol{F}_E =& \bar{\mathbf{J}}^{\#T}\boldsymbol{\tau}_E.
\end{aligned}$$

The internal motion of the manipulator subjected to the torque applied through the null space of $\mathbf{J}^T$ can be described by the following equation:

$$\bar{\mathbf{N}}^T\boldsymbol{\tau} = \bar{\mathbf{N}}^T\mathbf{H}\bar{\mathbf{N}}\ddot{\boldsymbol{q}} + \bar{\mathbf{N}}^T(\mathbf{C}\dot{\boldsymbol{q}} + \boldsymbol{g}) - \bar{\mathbf{N}}^T\boldsymbol{\tau}_E.$$

The matrix, which premultiplies $\ddot{\boldsymbol{q}}$, and is defined as

$$\mathbf{H}_n = \bar{\mathbf{N}}^T\mathbf{H}\bar{\mathbf{N}} = \mathbf{H} - \mathbf{J}^T\mathbf{M}\mathbf{J}$$

will be denoted as the *null-space effective inertia matrix*. The matrix $\mathbf{H}_n$ describes the inertial properties of the system in the null space. As $\mathbf{H}_n$ has not a full rank, rank$(\mathbf{H}_n) < n$, we define the generalized inverse of the null-space effective inertia matrix $\mathbf{H}_n$ as

$$\mathbf{H}_n^{\ddagger} = \bar{\mathbf{N}}\mathbf{H}^{-1}\bar{\mathbf{N}}^T.$$

Note that $\mathbf{H}_n^{\ddagger}\mathbf{H}_n\mathbf{H}_n^{\ddagger} = \mathbf{H}_n^{\ddagger}$, $\mathbf{H}_n\mathbf{H}_n^{\ddagger}\mathbf{H}_n = \mathbf{H}_n$ and $\mathbf{H}_n^{\ddagger} = (\mathbf{H}_n^{\ddagger})^T$.

V. Control Algorithms

Most of the tasks performed by a redundant manipulator can be broken down into several subtasks with different priorities. In the following it is assumed that the subtask with the highest priority, referred to as the main task, is associated with the positioning of the end-effector and the force acting on the end-effector, and the secondary task is to track a prescribed null-space velocity.

Utilizing a formulation of the generalized forces, a control law is given in the form

$$\boldsymbol{\tau} = \mathbf{J}^T\mathbf{M}\left(\ddot{\boldsymbol{x}}_c - \dot{\mathbf{J}}\dot{\boldsymbol{q}}\right) + \bar{\mathbf{N}}^T\mathbf{H}\left(\boldsymbol{\phi} + \dot{\bar{\mathbf{J}}}\dot{\boldsymbol{x}}\right) + \mathbf{C}\dot{\boldsymbol{q}} + \boldsymbol{g} + \mathbf{J}^T\boldsymbol{F}_E \tag{11}$$

where $\ddot{\boldsymbol{x}}_c$ and $\boldsymbol{\phi}$ represent the control law for the task motion and internal motion, respectively, and $\boldsymbol{F}_E$ is the task-space force measured at the robot's tool center point (TCP) using the force/torque sensor. The closed-loop dynamics are obtained by inserting the above equation into (9)

$$\mathbf{H}\ddot{\boldsymbol{q}} - \boldsymbol{\tau}_E = \mathbf{J}^T\mathbf{M}\left(\ddot{\boldsymbol{x}}_c - \dot{\mathbf{J}}\dot{\boldsymbol{q}}\right) + \bar{\mathbf{N}}^T\mathbf{H}\left(\boldsymbol{\phi} + \dot{\bar{\mathbf{J}}}\dot{\boldsymbol{x}}\right) + \mathbf{J}^T\boldsymbol{F}_E. \tag{12}$$

Next, we will analyze the behavior of the proposed controller in the task space and null space independently. Premultiplying (12) by $\mathbf{J}\mathbf{H}^{-1}$ and considering $\ddot{\boldsymbol{x}} = \mathbf{J}\ddot{\boldsymbol{q}} + \dot{\mathbf{J}}\dot{\boldsymbol{q}}$ yields

$$\begin{aligned}
\ddot{\boldsymbol{x}}_c - \ddot{\boldsymbol{x}} =& \bar{\mathbf{J}}\mathbf{H}^{-1}\left(\mathbf{J}^T\boldsymbol{F}_E - \boldsymbol{\tau}_E\right) \\
=& \bar{\mathbf{J}}\mathbf{H}^{-1}\bar{\mathbf{N}}^T\boldsymbol{\tau}_E \\
=& 0
\end{aligned} \tag{13}$$

since $\mathbf{J}\mathbf{H}^{-1}\mathbf{J}^T\mathbf{M} = \mathbf{I}$ and $\mathbf{J}\mathbf{H}^{-1}\bar{\mathbf{N}}^T = 0$.

Similarly, null-space dynamics can be obtained by premultiplying (12) with $\bar{\mathbf{N}}\mathbf{H}^{-1}$

$$\begin{aligned}
\bar{\mathbf{N}}\ddot{\boldsymbol{q}} - \bar{\mathbf{N}}\mathbf{H}^{-1}\bar{\mathbf{N}}^T\boldsymbol{\tau}_E = \bar{\mathbf{N}}\mathbf{H}^{-1}\mathbf{J}^T\mathbf{M}\left(\ddot{\boldsymbol{x}}_c - \dot{\mathbf{J}}\boldsymbol{q}\right) \\
+ \bar{\mathbf{N}}\mathbf{H}^{-1}\bar{\mathbf{N}}^T\mathbf{H}\left(\boldsymbol{\phi} + \dot{\mathbf{J}}^{\#}\dot{\boldsymbol{x}}\right).
\end{aligned} \tag{14}$$

Considering that $\bar{\mathbf{N}}\mathbf{H}^{-1}\bar{\mathbf{N}}^T\mathbf{H} = \bar{\mathbf{N}}$ and $\bar{\mathbf{N}}\mathbf{H}^{-1}\mathbf{J}^T\mathbf{M} = 0$, we obtain

$$\bar{\mathbf{N}}\left(-\ddot{\boldsymbol{q}} + \boldsymbol{\phi} + \dot{\bar{\mathbf{J}}}\dot{\boldsymbol{x}}\right) = -\mathbf{H}_n^{\ddagger}\boldsymbol{\tau}_E. \tag{15}$$

A. Task-Space Controller

Let $\ddot{\boldsymbol{x}}_c$ be selected as

$$\ddot{\boldsymbol{x}}_c = \ddot{\boldsymbol{x}}_d + \mathbf{K}_v\dot{\boldsymbol{e}} + \mathbf{K}_p\boldsymbol{e} + \mathbf{K}_f\left(\boldsymbol{F}_d - \boldsymbol{F}_E\right) \tag{16}$$

where $\boldsymbol{e}$, $\boldsymbol{e} = \boldsymbol{x}_d - \boldsymbol{x}$, is the tracking error, $\ddot{\boldsymbol{x}}_d$ is the desired task-space acceleration, and $\mathbf{K}_v$, $\mathbf{K}_p$ and $\mathbf{K}_f$ are $n \times n$ constant gain matrices. The selection of $\mathbf{K}_v$, $\mathbf{K}_p$, and $\mathbf{K}_f$ can be based on the desired task-space impedance. $\boldsymbol{F}_d$ denotes the desired external force. It is supposed that the external force $\boldsymbol{F}_E$ can be measured by an appropriate force/torque sensor. Substituting (16) for $\ddot{\boldsymbol{x}}_c$ in (13) yields

$$\ddot{\boldsymbol{e}} + \mathbf{K}_v\dot{\boldsymbol{e}} + \mathbf{K}_p\boldsymbol{e} = -\mathbf{K}_f\left(\boldsymbol{F}_d - \boldsymbol{F}_E\right).$$

As we can see, the task-space impedance can be chosen freely. By selecting $\mathbf{K}_v = \mathbf{M}_d^{-1}\mathbf{D}_d$, $\mathbf{K}_p = \mathbf{M}_d^{-1}\mathbf{K}_d$, and $\mathbf{K}_f'' = \mathbf{M}_d^{-1}\mathbf{K}_f$ the following task-space impedance can be achieved:

$$\mathbf{M}_d\ddot{\boldsymbol{e}} + \mathbf{D}_d\dot{\boldsymbol{e}} + \mathbf{K}_d\boldsymbol{e} = -\mathbf{K}_f''\left(\boldsymbol{F}_d - \boldsymbol{F}_E\right).$$

$\mathbf{M}_d$, $\mathbf{D}_d$, and $\mathbf{K}_d$ are the desired task space inertia, damping, and stiffness matrices, respectively.

B. Null-Space Controller

Besides the main task, a redundant system can perform an additional subtask by selecting an appropriate vector $\boldsymbol{\phi}$ in the control law (11) which moves the manipulator toward the desired configuration. Let $\dot{\boldsymbol{\varphi}}_n$ be the desired null-space velocity,

$\dot{\boldsymbol{\varphi}}_n = \bar{\mathbf{N}}\dot{\boldsymbol{\varphi}}$. To obtain good tracking of $\dot{\boldsymbol{\varphi}}_n$ in the null space, the following $\boldsymbol{\phi}$ is proposed [14]:

$$\boldsymbol{\phi} = \ddot{\boldsymbol{\varphi}}_n + k_n\dot{\boldsymbol{e}}_n + \mathbf{H}^{-1}\mathbf{C}\dot{\boldsymbol{e}}_n = \bar{\mathbf{N}}\ddot{\boldsymbol{\varphi}} + \dot{\bar{\mathbf{N}}}\dot{\boldsymbol{\varphi}} + k_n\dot{\boldsymbol{e}}_n + \mathbf{H}^{-1}\mathbf{C}\dot{\boldsymbol{e}}_n \tag{17}$$

where $\dot{\boldsymbol{e}}_n = \bar{\mathbf{N}}(\dot{\boldsymbol{\varphi}} - \dot{\boldsymbol{q}})$ and k_n is the positive scalar describing feedback gain. Substituting (17) into (15) yields

$$\bar{\mathbf{N}}\left(\ddot{\boldsymbol{\varphi}} - \ddot{\boldsymbol{q}}\right) = \bar{\mathbf{N}}\left(-\mathbf{H}^{-1}\mathbf{C}\dot{\boldsymbol{e}}_n - k_n\dot{\boldsymbol{e}}_n - \dot{\bar{\mathbf{N}}}\dot{\boldsymbol{\varphi}} - \dot{\bar{\mathbf{J}}}\dot{\boldsymbol{x}}\right) - \mathbf{H}_n^{\ddagger}\boldsymbol{\tau}_E. \tag{18}$$

Differentiating $\dot{\boldsymbol{e}}_n$ results in

$$\ddot{\boldsymbol{e}}_n = \bar{\mathbf{N}}\left(\ddot{\boldsymbol{\varphi}} - \ddot{\boldsymbol{q}}\right) + \dot{\bar{\mathbf{N}}}\left(\dot{\boldsymbol{\varphi}} - \dot{\boldsymbol{q}}\right). \tag{19}$$

Using (18) in the above equation yields

$$\ddot{\boldsymbol{e}}_n = -\bar{\mathbf{N}}\mathbf{H}^{-1}\mathbf{C}\dot{\boldsymbol{e}}_n - \bar{\mathbf{N}}k_n\dot{\boldsymbol{e}}_n - \dot{\bar{\mathbf{N}}}\dot{\boldsymbol{q}} - \bar{\mathbf{N}}\dot{\bar{\mathbf{J}}}\dot{\boldsymbol{x}} - \mathbf{H}_n^{\ddagger}\boldsymbol{\tau}_E. \tag{20}$$

Note that $\dot{\boldsymbol{\varphi}}$ belongs to the null space of $\mathbf{J}$ and $\bar{\mathbf{N}}\dot{\bar{\mathbf{J}}}\dot{\boldsymbol{x}} = -\bar{\mathbf{N}}\dot{\bar{\mathbf{N}}}\dot{\boldsymbol{q}}$. This can be verified by

$$\bar{\mathbf{N}}\dot{\bar{\mathbf{N}}}\dot{\boldsymbol{q}} = -\bar{\mathbf{N}}\left(\bar{\mathbf{J}}\dot{\mathbf{J}} + \dot{\bar{\mathbf{J}}}\mathbf{J}\right)\dot{\boldsymbol{q}} = -\bar{\mathbf{N}}\dot{\bar{\mathbf{J}}}\dot{\boldsymbol{x}}$$

since $\bar{\mathbf{N}}\bar{\mathbf{J}} = 0$. Hence, (20) can be rewritten in the form

$$\ddot{\boldsymbol{e}}_n = -\bar{\mathbf{N}}\mathbf{K}_n\dot{\boldsymbol{e}}_n - \bar{\mathbf{N}}\mathbf{H}^{-1}\mathbf{C}\dot{\boldsymbol{e}}_n - (\mathbf{I} - \bar{\mathbf{N}})\dot{\bar{\mathbf{N}}}\dot{\boldsymbol{q}} - \mathbf{H}_n^{\ddagger}\boldsymbol{\tau}_E. \tag{21}$$

Next, we show that for $\mathbf{N}^T\boldsymbol{\tau}_E = 0$, the proposed control method (17) assures asymptotic stability of the system in the null space and that the $\dot{\boldsymbol{e}}$ converges to zero. In this case, the last term $\mathbf{H}_n^{\ddagger}\boldsymbol{\tau}_E$ in (20) is equal to zero. Let the Lyapunov function be defined as $v = 1/2\ \dot{\boldsymbol{e}}_n^T\mathbf{H}\dot{\boldsymbol{e}}_n$. Differentiating v and substituting (21) for $\ddot{\boldsymbol{e}}$ yields

$$\begin{aligned}\dot{v} =& \dot{\boldsymbol{e}}_n^T\mathbf{H}\ddot{\boldsymbol{e}}_n + \frac{1}{2}\dot{\boldsymbol{e}}_n^T\dot{\mathbf{H}}\dot{\boldsymbol{e}}_n\\ =& -\dot{\boldsymbol{e}}_n^T\mathbf{H}\bar{\mathbf{N}}k_n\dot{\boldsymbol{e}}_n - \dot{\boldsymbol{e}}_n^T\mathbf{H}\bar{\mathbf{N}}\mathbf{H}^{-1}\mathbf{C}\dot{\boldsymbol{e}}_n - \dot{\boldsymbol{e}}_n^T\mathbf{H}(\mathbf{I} - \bar{\mathbf{N}})\dot{\bar{\mathbf{N}}}\dot{\boldsymbol{q}}\\ &+ \frac{1}{2}\dot{\boldsymbol{e}}_n^T\dot{\mathbf{H}}\dot{\boldsymbol{e}}_n\\ =& \dot{\boldsymbol{e}}_n^T\mathbf{H}k_n\dot{\boldsymbol{e}}_n - \dot{\boldsymbol{e}}_n^T\mathbf{H}(\mathbf{I} - \bar{\mathbf{J}}\mathbf{J})\mathbf{H}^{-1}\mathbf{C}\dot{\boldsymbol{e}}_n - \dot{\boldsymbol{e}}_n^T\mathbf{H}(\bar{\mathbf{J}}\mathbf{J})\dot{\bar{\mathbf{N}}}\dot{\boldsymbol{q}}\\ &+ \frac{1}{2}\dot{\boldsymbol{e}}_n^T\dot{\mathbf{H}}\dot{\boldsymbol{e}}_n\\ =& -k_n\dot{\boldsymbol{e}}_n^T\mathbf{H}\dot{\boldsymbol{e}}_n - \frac{1}{2}\dot{\boldsymbol{e}}_n^T(\dot{\mathbf{H}} - 2\mathbf{C})\dot{\boldsymbol{e}}_n\\ =& -k_n\dot{\boldsymbol{e}}_n^T\mathbf{H}\dot{\boldsymbol{e}}_n\end{aligned} \tag{22}$$

since $\dot{\boldsymbol{e}}_n^T\mathbf{H}\bar{\mathbf{J}} = 0$, $\bar{\mathbf{N}}\dot{\boldsymbol{e}}_n = \dot{\boldsymbol{e}}_n$, and $(\dot{\mathbf{H}} - 2\mathbf{C})$ is skew symmetric. Since v is positive definite and $\dot{v}$ is negative definite providing that k_n is positive scalar, $\dot{\boldsymbol{e}}_n$ tends to zero, and the proposed controller stabilizes the null-space motion as long as the Jacobian is nonsingular. Note that the matrix $\dot{\mathbf{H}} - 2\mathbf{C}$ is skew symmetric only if $\mathbf{C}(\boldsymbol{q}, \dot{\boldsymbol{q}})$ is formed using Christoffel terms. A similar result has been independently derived in [3].

Null-space dynamics can be obtained from (21)

$$\begin{aligned}\mathbf{H}_n\ddot{\boldsymbol{e}}_n =& -\bar{\mathbf{N}}^T\mathbf{H}\bar{\mathbf{N}}\bar{\mathbf{N}}k_n\dot{\boldsymbol{e}}_n - \bar{\mathbf{N}}^T\mathbf{H}\bar{\mathbf{N}}\bar{\mathbf{N}}\mathbf{H}^{-1}\mathbf{C}\dot{\boldsymbol{e}}_n\\ &- \bar{\mathbf{N}}^T\mathbf{H}\bar{\mathbf{N}}(\mathbf{I} - \bar{\mathbf{N}})\dot{\bar{\mathbf{N}}}\dot{\boldsymbol{q}} - \bar{\mathbf{N}}^T\mathbf{H}\bar{\mathbf{N}}\mathbf{H}_n^{\ddagger}\boldsymbol{\tau}_E.\end{aligned} \tag{23}$$

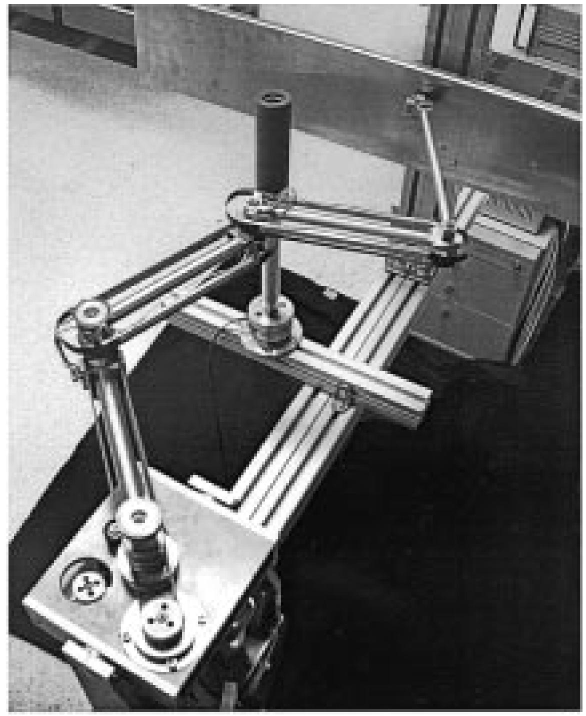

Fig. 1. 4-DOF experimental robot.

Since $\bar{\mathbf{N}}$ is idempotent, $\bar{\mathbf{N}}\bar{\mathbf{N}} = \bar{\mathbf{N}}$, it follows $\bar{\mathbf{N}}(\mathbf{I} - \bar{\mathbf{N}}) = 0$, $\mathbf{H}\bar{\mathbf{N}} = \bar{\mathbf{N}}^T\mathbf{H}$. Using the definition of $\mathbf{H}_n^{\ddagger}$, (23) can be expressed in the form

$$\mathbf{H}_n\ddot{\boldsymbol{e}}_n + (\mathbf{H}_n\mathbf{K}_n + \bar{\mathbf{N}}^T\mathbf{C})\dot{\boldsymbol{e}}_n = -\bar{\mathbf{N}}^T\boldsymbol{\tau}_E. \tag{24}$$

The above equation describes the null space dynamics. Summarizing, the control method (17) enables the selection of the damping by selecting $\mathbf{K}_n$.

VI. Null-Space Motion Optimization

The force and the position tracking are usually of the highest priority for a force-controlled robot. The selection of the subtasks with lower priority depends on the specific application [4]. However, collision avoidance is of great importance, since the force-controlled robot interacts with the environment. In our previous work, we implemented the obstacle avoidance algorithm using potential field. This approach requires the distance between the obstacle and any part of the robot. Besides being time consuming, this approach requires at least the approximate position of the environment obstacle. Here, we assume that this information is not known and cannot be obtained. Therefore, we allow the robot to bump into obstacles, but we try to minimize the resulting forces by adopting the null-space dynamics.

An important subtask for the force-controlled robot might be to benefit the mechanical advantage of the manipulator in order to minimize joint torques when applying a certain force to the end-effector. The local joint torque minimization as a performance objective was intensively investigated by many authors [2], [6], [7]. As the joint torque depends on the system dynamics, it is difficult to express the gradient of the cost function related to joint torques. We simplified the problem by minimizing only

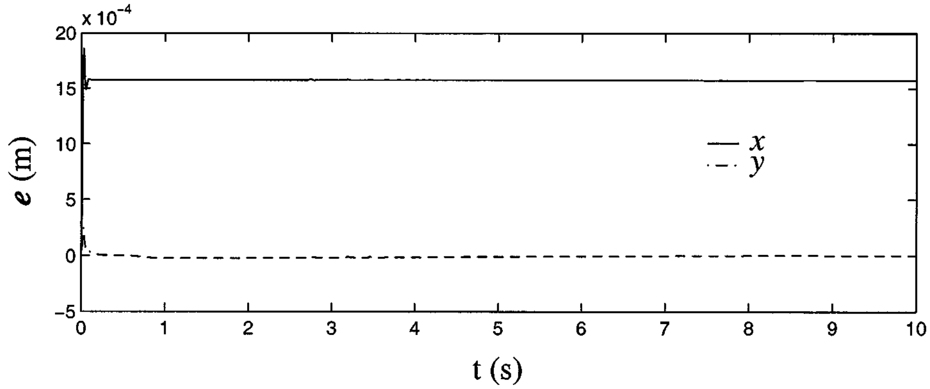

Fig. 2. Simulated TCP tracking error.

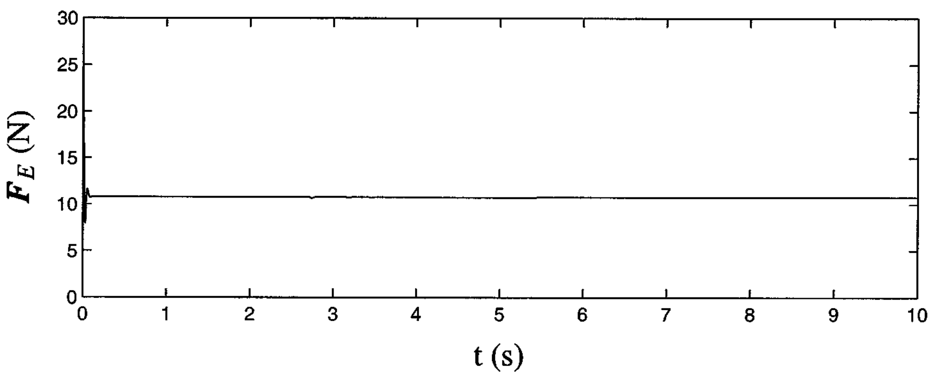

Fig. 3. Simulated TCP force.

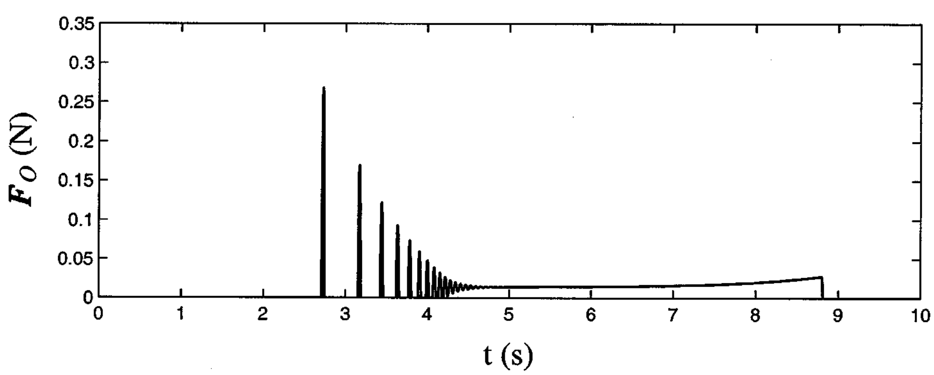

Fig. 4. Simulated obstacle force.

joint torques related to the force applied to the robot end-effector. We define the cost function in the form $\boldsymbol{p} = \boldsymbol{\tau}^T\boldsymbol{\tau}$, where $\boldsymbol{\tau} = \mathbf{J}^T\boldsymbol{F}_E$ is the joint torque due to the end-effector force. Then, the cost function gradient required to minimize the given function can be expressed in the form

$$\frac{\partial \boldsymbol{p}}{\partial \boldsymbol{q}} = 2\boldsymbol{F}^T\mathbf{J}\nabla\boldsymbol{\tau}, \tag{25}$$

$$\nabla\boldsymbol{\tau} = \begin{bmatrix} \frac{\partial \mathbf{J}^{(1)}}{\partial \boldsymbol{q}_1}\boldsymbol{F} & \frac{\partial \mathbf{J}^{(1)}}{\partial \boldsymbol{q}_2}\boldsymbol{F} & \cdots & \frac{\partial \mathbf{J}^{(1)}}{\partial \boldsymbol{q}_n}\boldsymbol{F} \\ \frac{\partial \mathbf{J}^{(2)}}{\partial \boldsymbol{q}_1}\boldsymbol{F} & \frac{\partial \mathbf{J}^{(2)}}{\partial \boldsymbol{q}_2}\boldsymbol{F} & \cdots & \frac{\partial \mathbf{J}^{(2)}}{\partial \boldsymbol{q}_n}\boldsymbol{F} \\ \vdots & \vdots & \vdots & \vdots \\ \frac{\partial \mathbf{J}^{(n)}}{\partial \boldsymbol{q}_1}\boldsymbol{F} & \frac{\partial \mathbf{J}^{(n)}}{\partial \boldsymbol{q}_2}\boldsymbol{F} & \cdots & \frac{\partial \mathbf{J}^{(n)}}{\partial \boldsymbol{q}_n}\boldsymbol{F} \end{bmatrix} \tag{26}$$

where $\mathbf{J}^{(i)}$ denotes the ith column of the Jacobian $\mathbf{J}$. This approach can be justified by the fact that velocities and accelera-tion during the force tracking are usually low. Another advantage using this approach is that the minimization can be related to the desired end-effector force and the manipulator can be brought to the optimal pose before the contact with the environment is established.

The desired null-space velocities can be obtained utilizing modified gradient optimization procedure

$$\dot{\varphi} = \bar{\mathbf{J}}\dot{\boldsymbol{x}} + \bar{\mathbf{N}}k_o\mathbf{H}^{-1}\psi \tag{27}$$

which assures the best optimization step in the case of inertia weighted pseudoinverse. k_o defines the optimization step. Vector ψ is a gradient optimization vector defined as

$$\psi = \left(\frac{\partial \boldsymbol{p}}{\partial q_1}, \frac{\partial \boldsymbol{p}}{\partial q_2}, \ldots, \frac{\partial \boldsymbol{p}}{\partial q_N}\right)^T. \tag{28}$$

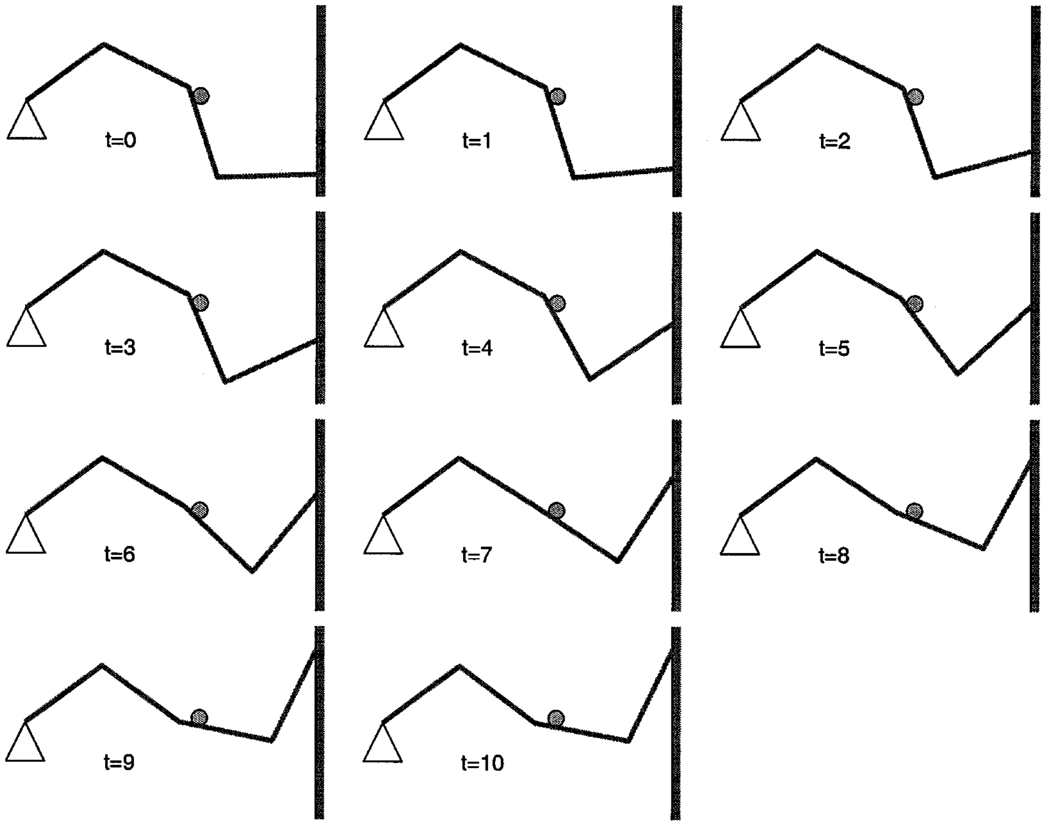

Fig. 5. Poses of the robot during the simulation of the task.

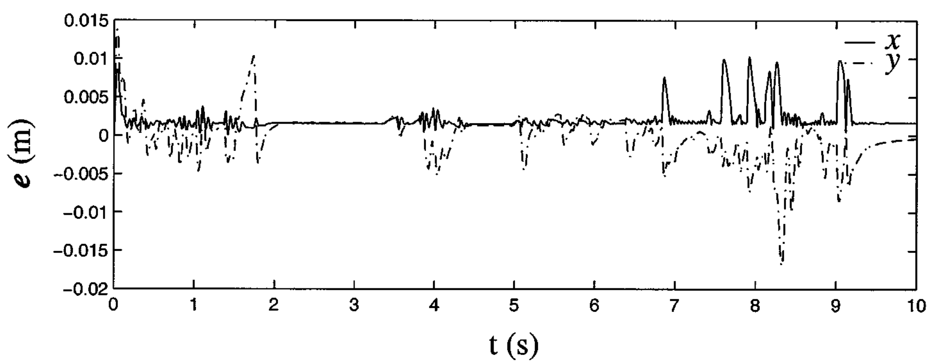

Fig. 6. TCP tracking error.

Unfortunately, the local joint torque minimization often brings the robot into the singular configuration. Therefore, the singularity avoidance algorithm also has to be implemented. We have accomplished this task by maximizing manipulator manipulability proposed by [17].

VII. Experiments

The efficiency of the proposed algorithm was tested on a 4-DOF planar redundant robot with all segments of equal length, presented in Fig. 1. The robot had no limits in joint angles. All ac brushless motors were located in the robot base in order to obtain lightweight links. The robot gear ratio was 6, thus, the coupled dynamics of the robot are not negligible. We used two JR3 force sensors, capable of measuring three forces and three torques. One sensor was used for force tracking and the other for measuring contact force with an obstacle. The sensor used for force tracking was too heavy to be carried by the experimental robot, therefore, we mounted the sensor under the environment plane. The obstacle was a vertical bar mounted on the force sensor. Forces from this sensor were used to measure the contact forces between the robot and the obstacle. The robot controller consists of a Pentium II 360-MHz industrial computer. The proposed control algorithm was realized in SIMULINK and compiled using the Simulink Real Time Workshop and Planar Manipulator Toolbox.

The primary task of the manipulator was to track the desired force while moving along the wall in the horizontal (x) direction. The desired speed was 0.45 m/s and the desired force was 10 N. There was an obstacle in the robot workspace, as shown in

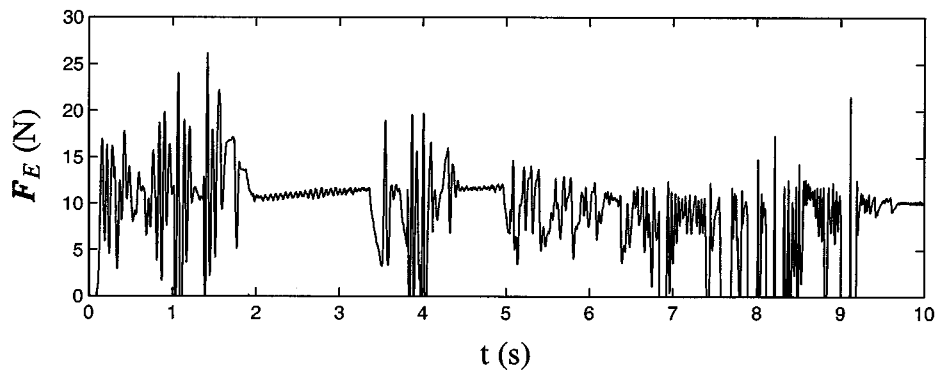

Fig. 7. TCP force.

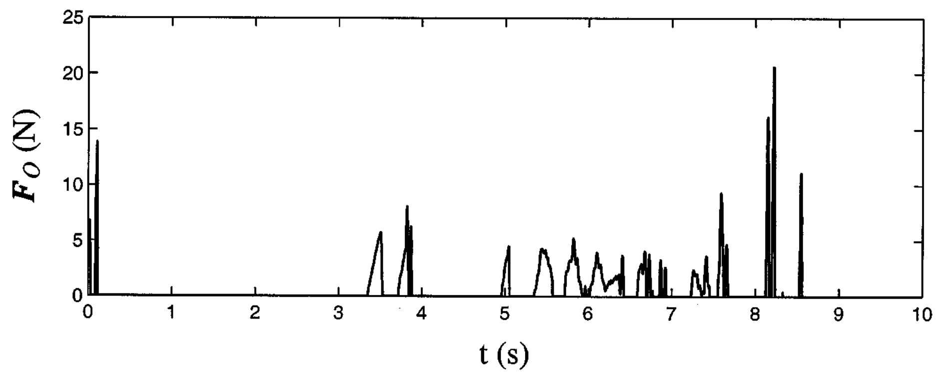

Fig. 8. Obstacle force.

Fig. 5. The position of the obstacle and the contact forces were not known in the control law. The secondary subtasks were minimization of contact forces, minimization of the joint torques due to the end-effector force and maximization of the manipulability index. Because the impact was not the issue, we started the experiment with the robot in contact with the wall.

First, we tested the proposed control law using the simulation. The simulation results of position tracking, force tracking, and obstacle force are presented in Figs. 2–4, respectively. Fig. 5 shows poses of the robot in subsequent time intervals. From the results, we can see that the obstacle contact forces had virtually no influence on the primary task, which was force and trajectory tracking. By selecting the appropriate null-space dynamics, contact forces were minimized.

We repeated the same task on the real robot. We obtained a control rate of 500 Hz. The results are presented in Figs. 6–8. In this case, we can notice the influence of the contact force with the obstacle to the TCP tracking error and TCP force. The performance degradation is mainly due to the elasticity of the gear belts and gear friction. Although we included a nonlinear friction compensator in the control loop, it was not possible to cancel the friction effect.

VIII. CONCLUSION

This paper has considered the force control of redundant robots in the presence of unknown obstacles. Instead of an obstacle avoidance algorithm, we have changed the dynamics properties of the redundant manipulator in order to minimize the impact forces. Therefore, special attention was given to the dynamic decoupling and the inertial properties of the system in the space where internal motion is taking place; we defined a *null-space effective inertia* and its inverse. Finally, we proposed a control algorithm (11) which decouples the motion of the manipulator into the end-effector motion and the internal motion. The controller enables the selection of dynamic characteristics in both subspaces separately. The proposed algorithm was tested using the simulation and on the real robot. With the simulation results, we showed that we have successfully decoupled null-space and task-space dynamics. A disturbance, caused by the obstacle, has virtually no effect on the primary task. Experiments on the real robot show similar results, but the performance is degraded by the elasticity and the friction in the robot joints. On the other hand, compliant dynamics require low null-space gains, which limit the performance of the null-space tracking algorithm.

REFERENCES

[1] H. Asada and J.-J Slotine, *Robot Analysis and Control*. New York: Wiley, 1986.
[2] T. Chen, F. Cheng, Y. Sun, and M. Hung, “Torque optimization schemes for kinematically redundant manipulators,” *J. Robot. Syst.*, vol. 11, no. 4, pp. 258–269, 1994.
[3] C. Natale, B. Siciliano, and L. Vilani, “Spatial impedance control of redundant manipulators,” in *Proc. IEEE Int. Symp. Robotics and Automation, ICRA’99*, Detroit, MI, 1999, pp. 1788–1793.
[4] R. Dubey and J. Luh, “Redundant robot control using task based performance measures,” *J. Robot. Syst.*, vol. 5, no. 5, pp. 409–432, 1988.
[5] R. Featherstone and O. Khatib, “Load independance of the dynamically consistent inverse of the Jacobian Matrix,” *Int. J. Robot. Res.*, vol. 16, no. 2, pp. 168–170, 1997.

[6] J. M. Hollerbach and K. C. Suh, "Redundancy resolution of manipulators through torque optimization," *IEEE Trans. Robot. Automat.*, vol. RA-3, pp. 308–316, Aug. 1987.

[7] H. Kang and R. Freeman, "Null space damping method for local joint torque optimization of redundant manipulators," *J. Robot. Syst.*, vol. 10, no. 2, pp. 249–270, 1993.

[8] O. Khatib, "A unified approach for motion and force control of robot manipulators: The operational space formulation," *IEEE Trans. Robot. Automat.*, vol. 3, pp. 43–53, Feb. 1987.

[9] ——, "The impact of redundancy on the dynamic performance of robots," *Lab. Robot. Automat.*, vol. 8, no. 1, pp. 37–48, 1996.

[10] C. A. Klein and C. H. Huang, "Review of pseudoinverse control for use with kinematically redundant manipulators," *IEEE Trans. Syst., Man, Cybern.*, vol. SMC-13, pp. 245–250, Mar./Apr. 1983.

[11] J. Luh, "Convetional controller design for industrial robots—a tutorial," *IEEE Trans. Syst., Man, Cybern.*, vol. SMC-13, pp. 298–316, Mar. 1983.

[12] J. Luh, M. Walker, and R. Paul, "Resolved acceleration control of mechanical manipulators," *IEEE Trans. Automat. Contr.*, vol. AC-25, pp. 486–474, June 1980.

[13] A. Maciejewski, "Kinetic limitations on the use of redundancy in robotic manipulators," *IEEE Trans. Robot. Automat.*, vol. 7, pp. 205–201, Mar. 1991.

[14] B. Nemec and L.Žlajpah, "Experiments on impedance control of redundant manipulators," in *Proc. IEEE Int. Symp. Industrial Electronics, ISIE'99*, Bled, Slovenia, 1999, pp. 134–138.

[15] D. N. Nenchev, "Redundancy resolution through local optimization: A review," *J. Robot. Syst.*, vol. 6, no. 6, pp. 769–798, 1989.

[16] J. Park, W. Chung, and Y. Youm, "Weighted decomposition of kinematics and dynamics of kinematically redundant manipulators," in *Proc. IEEE Conf. Robotics and Automation*, 1996, pp. 480–486.

[17] T. Yoshikawa, *Foundations of Robotics: Analysis and Control*. Cambridge, MA: MIT Press, 1990.

Bojan Nemec received the B.Sc., M.Sc., and D.Sc. degrees from the University of Ljubljana, Ljubljana, Slovenia, in 1979, 1982, and 1988, respectively.

From 1979 to 1982, he was with the Faculty of Electrical Engineering, University of Ljubljana, as a Research Assistant. In 1983, he joined the Department of Automatics, Biocybernetics and Robotics, Jožef Stefan Institute, Ljubljana, Slovenia. In 1993, he studied at the Institute for Real-Time Computer Systems and Robotics, University of Karlsruhe, Germany. His research interests includes robot control, sensor-guided control, and biomechanical measurements in sport.

Leon Žlajpah received the B.Sc. degree in automatics, the M.Sc. degree, and the Ph.D. degree in electrical science from the University of Ljubljana, Ljubljana, Slovenia, in 1982, 1985, and 1989, respectively.

Since 1981, he has been with the Department of Automatics, Biocybernetics and Robotics, Jozef Stefan Institute, Ljubljana, Slovenia, working in different fields of robotics. Since 1998, he has been a Senior Researcher. His fields of interest include intelligent control, in particular, analysis and synthesis of control systems for redundant robots, sensors, applications, computer-integrated manufacturing, and modeling of dynamic systems and their simulation.

Dr. Zlajpah is member of the Slovenian Society for Simulation and Modeling, Automatics Society of Slovenia, and Robotics Society of Slovenia.